International Scientific Conference 20 UNITECH 26

INTERNATIONAL SCIENTIFIC CONFERENCE
19-21 November 2026
GABROVO

AN IN-SILICO STUDY OF IMIDAZOPHENANTHROLINE-DERIVED LIGAND: CHARACTERIZATION AND MOLECULAR DOCKING APPROACH

G. Uluçam

Chemistry Department, Faculty of Science, Trakya University, Edirne, Türkiye
Corresponding author: e-mail: gulergul@trakya.edu.tr

Abstract
Heterocyclic and bicyclic structural units are commonly seen in biologically active molecules. Imidazophenanthrolines are nitrogen-containing heterocyclic molecules characterized by an imidazole ring fused to a phenanthroline ring, ranked among the frequently searched constituents in the pharmaceutical industry. Imidazophenanthrolines are notable for their anticancer, antifungal, and antimicrobial effects. In this study, imidazophenanthroline-derived ligand (4-((1*H*-imidazo[4,5-*f*][1,10]phenanthrolin-1-yl)methyl)phenol) was optimized using the B3LYP/6-311G++ (2d, p) basis set in the Gaussian G09w software package, and their theoretical properties were investigated. Then, the potential interactions of the ligand with selected target proteins were evaluated using molecular docking, which is an in-silico computational technique used to predict the nature of potential interactions between a ligand and a targeted receptor and to visualize the model of this target binding. The target proteins were identified using the Swiss Target Prediction (swisstargetprediction.ch) online tool, and the top proteins showing the highest potential were selected as targets. Molecular docking analyses were performed using AutoDockTools Version 1.5.6 (September 17, 2014); the binding energies, interaction sites, and interaction types of the imidazophenanthroline-derived ligand with the target proteins were determined and evaluated.

Keywords: *Imidazophenanthroline, BRD4, CYP11B2, DFT/B3LYP*

INTRODUCTION

1,10-Phenanthroline (phen) is a classic bidentate ligand that has played a pivotal role in the evolution of coordination chemistry and continues to attract significant interest today as a versatile starting material in the fields of organic, inorganic, and supramolecular chemistry. Phen is a rigid, planar, hydrophobic, and electron-deficient heteroaromatic structure featuring nitrogen atoms ideally positioned to participate in cation binding. These structural attributes define its coordination capacity toward metal ions. The 5- and 6-positions of the phen structure are the most favorable sites for electrophilic substitution reactions. 1*H*-Imidazo[4,5-*f*][1,10]-phenanthroline (IP) is a significant constituent of the phen structure. Containing aromatic/hetero rings, IP enables delicate π–π stacking interactions to play a crucial role in the formation of supramolecular structures; this characteristic is vital for complex formation and stabilization and is also a significant factor influencing catalytic activity [1]. IP derivative have a wide range of applications, particularly in the pharmaceutical industry [2-7]. Molecular docking is an in-silico computational technique used to predict the nature of potential interactions between a ligand and a targeted receptor and to visualize the model of this target binding. This method serves as a substantial tool in areas such as computer-aided drug design and the identification of target molecules for disease mechanisms in preclinical, in vivo, and in vitro experimental research.

In this study, imidazophenanthroline-derived ligand (4-((1*H*-imidazo[4,5-*f*][1,10] phenanthroline-1-yl)methyl)phenol) was

This is an open access article licensed under Creative Commons Attribution 4.0 International
Print ISSN: 1313-230X, Online ISSN: 3033-1404

optimized using the B3LYP/6-311G++ (2d, p) basis set in the Gaussian G09w [8] software package, and their theoretical properties were investigated.

Then, the potential interactions of the ligand with selected target proteins were evaluated using molecular docking. The target proteins were identified using the Swiss Target Prediction (swisstargetprediction.ch) online tool, and the top proteins showing the highest potential were selected as targets. Molecular docking analyses were performed using Auto Dock Tools Version 1.5.6 (September 17, 2014); the binding energies, interaction sites, and interaction types of the imidazophenanthroline-derived ligand with the target proteins were determined and evaluated.

FINDINGS

Molecular Geometry

The ligand was optimized in the gas phase, and its minimization energy, dipole moment, and polarizability were calculated as -1065.105364 au, 6.935847 Debye, and 282.1112 au, respectively. The ligand has the C1 symmetry group, and the structure of the ligand is shown in Fig. 1.

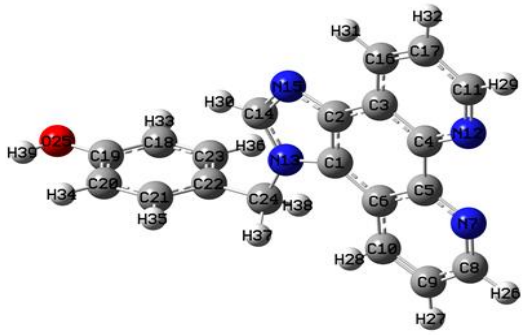


Fig. 1. *The suitable structure of the ligand with the lowest theoretically calculated energy.*

HOMO-LUMO Analysis and Electronic Properties

Frontier molecular orbitals (FMO) are dominant in determination the electrical and optical characteristics of a molecule. The energy difference between HOMO and LUMO provides information on the molecular properties. The diminished energy disparity leads to a more polarized molecule, which indicates a high reactivity.

Table 3*. Electronic structure parameters of the ligand and their values*

Parameter	***Value***
E_{HOMO} (eV)	-5.98732
E_{LUMO} (eV)	-1.60438
ΔE (eV)	4.38294
IP (eV)	5.98732
EA (eV)	1.60438
χ(eV)	3.79585
μ (eV)	-3.79585
η (eV)	2.19147
σ (eV^{-1})	0.45631
ω	3.28740

IP:-EHOMO, EA:-ELUMO, ΔE=ELUMO-EHOMO,

$\chi = (IP+EA)/2$, $\mu = -\chi$, $\eta = (IP-EA)/2$, $\sigma = 1/\eta$, $\omega = \mu^2/2\eta$

The energy of the Highest Occupied Molecular Orbital (HOMO) is associated with Ionization Potential (IP), while the energy of the Lowest Unoccupied Molecular Orbital (LUMO) corresponds to Electron Affinity (EA). Additionally, electronegativity (χ), chemical potential (μ), chemical hardness (η), electrophilicity index (ω), and chemical softness (σ) were calculated from FMO energies, as illustrated in Table 3. HOMO-LUMO energies in Fig. 2 [9, 10]. The Gaussian output values, articulated in atomic units (a. u.), were later converted into electrostatic units (1 a. u. = 27.211396 eV).

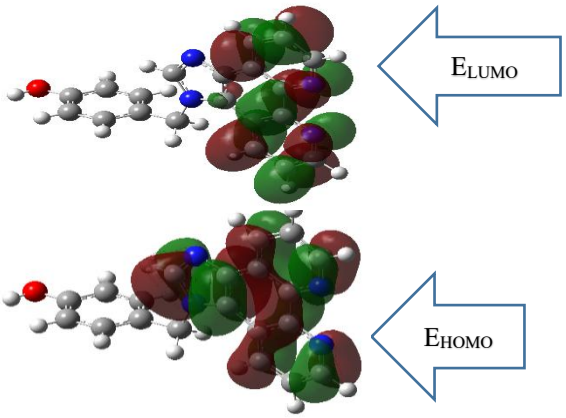


Fig. 2. *HOMO and LUMO three-dimensional representations and energy values*

The HOMO energy, indicative of the molecule's ability to donate electrons, is -

5.98732 eV, while the LUMO energy, indicating its electron removal potential, is -1.60438 eV; thus, the energy gap is calculated to be 4.38294 eV. The relatively small energy gap promotes the chemical synthesis of the molecule [11].

Theoretical NMR spectrums

The GIAO approach was employed to determine the theoretical ^{1}H- and ^{13}C-NMR chemical shifts, with the corresponding spectra illustrated in Fig. 3. and Figure 4.

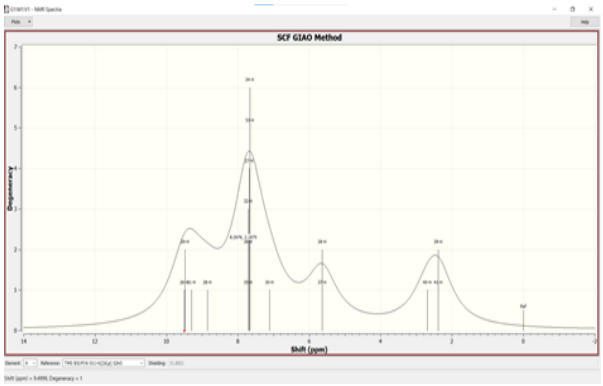


Fig. 3. *Theoretical ^{1}H-NMR spectra*

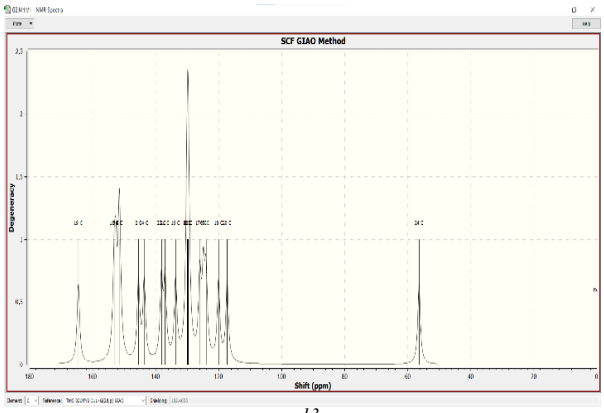


Fig. 5. *Theoretical ^{13}C-NMR spectra*

Chemical shift values for the protons in the ligand were determined as follows: aromatic protons between 9.48 and 6.87 ppm, the imidazole proton (H30) at 7.18 ppm, the CH_2 proton (H37, H38) at 5.58 ppm, and the OH proton (H39) at 4.03 ppm. For the carbons in the ligand, chemical shift values were determined as follows: aromatic carbons between 164.5 and 117.3 ppm, the imidazole carbon (C14) at 143.6 ppm, the CH2 carbon (C24) at 56.4 ppm, and OH's carbon (C19) at 164.5 ppm [12].

Theoretical FTIR spectrums

The calculated vibration spectrum is depicted in Fig. 5. It is commonly acknowledged that slight variations may occur between the vibration frequencies forecasted by quantum chemistry methods, such as DFT, and those measured in experiments. The inconsistencies are minimized by multiplying the theoretically calculated frequencies by 0.9613, the suitable scaling factor for the 6-311G++ (2d, p) basis set [12]. A comprehensive potential energy distribution (PED) analysis was conducted utilizing the VEDA software [13].



Fig. 5. *Theoretical FTIR spectrum*

An analysis of the ligand's theoretical FTIR spectrum disclosed 111 vibrational modes, including 38 stretching modes (ν), 37 bending modes (δ), and 36 torsional modes (γ). All vibration values are unscaled values.

The ν(O25H39) stretching mode was detected at 3824 cm^{-1}. All ν(CH) stretching modes appear in the 3261–3025 cm^{-1} range (specifically, imidazole ν(C14H30) at 3261 cm^{-1}, CH_2 asymmetric ν(C24H37, C224H38) at 3074 cm^{-1}, and CH_2 symmetric ν(C24H37, C224H38) at 3035 cm^{-1}). Selected vibrational modes (stretching, in-plane bending, and out-of-plane bending vibrations) are presented: the ν(N15C14) stretching mode is located at 1506 cm^{-1}, the ν(N7C8) and ν(N12C11) stretching modes at 1294 cm^{-1}, the ν(N7C8) stretching modes at 1366 cm^{-1}, the ν(N13C14) stretching mode at 1247 cm^{-1}, and the ν(C19C20) stretching mode at 1631 cm^{-1}; meanwhile, the δ(H34C20C21, H33C18C23, H36C23C22,

H35C21C22) bending mode is found at 1552 cm^{-1}, the δ(N13C14N15) bending mode at 1209 cm^{-1}, the δ(H30C14N15) bending mode at 1528 cm^{-1}, the δ(H39O25C19) bending mode at 1190 cm^{-1}, and the δ(C20C19O25) bending mode at 306 cm^{-1}. Additionally, the γ(H29C11N12C4, H31C16C3C4, H32C17C16C3) torsional mode was calculated at 1000 cm^{-1}, the γ(C2N15C14N13) torsional mode at 642 cm^{-1}, and the γ(O25C18C20C19) torsional mode at 513 cm^{-1}. A comparison of all calculated vibrational values with those from the literature indicates consistency [12, 13].

Molecular Docking

This is a theoretical computational method used to predict the preferred orientation of a ligand when it binds to a selected protein to form a stable complex. Molecular docking studies will be conducted using the Auto Dock Tools 1.5.6 software [14, 15]. The crystal structure of the selected protein will be obtained from the Protein Data Bank (CYP11B2 PDB ID:7M8V PDB DOI: https://doi.org/10.2210/pdb7M8V/pdb, BRD4 PDB ID: 7REK PDB DOI: https://doi.org/10.2210/pdb7REK/pdb) [16]. The protein will be prepared for analysis by removing surrounding water molecules and adding polar hydrogens and Kollman charges. A grid box will initially be set to maximum dimensions; once the interaction region is identified, the box size will be reduced to allow for a more detailed analysis. The ligand will be prepared for molecular docking after being energy-minimized using Gaussian G09w software. Following the analysis, interactions with the lowest energy levels will be selected for evaluation. The 2D and 3D structures of the binding site were visualized, and the types of interactions identified, using PyMOL and BIOVIA software [17].

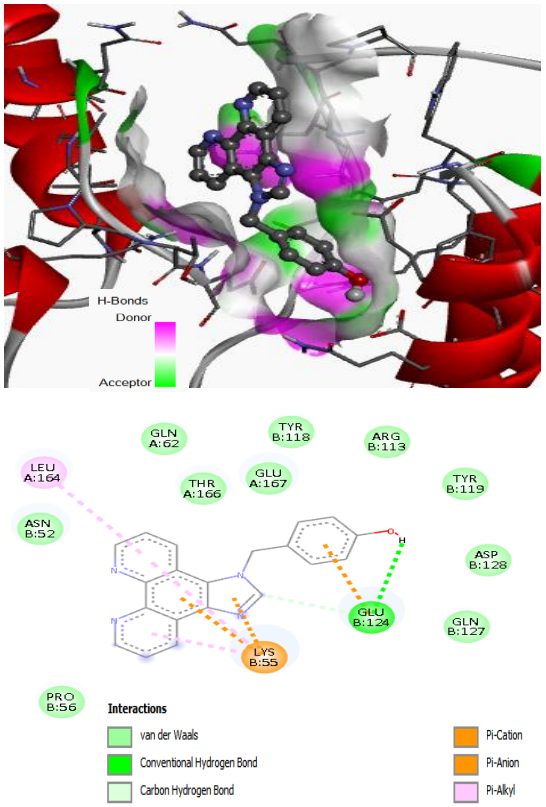


Fig. 6. *3D and 2D representation of the ligand-protein (CYP11B2) interaction site*

Table 4. *Interactions of the ligand with CYP11B2 and BRD4*

Docked Comp.	Interactions	Residues
CYP11B	Van der Waals	Asnb52, Glna62, Glua167, Tyrb118, Argb119, Tyrb119, Aspb128, Glnb127, Prob56, Thra66,
	Hydrogen bond	Glub124
	π-alkyl	Lysb55, Leua164
	C–H bond	Glub124
	π-cation	Lysb55, Glub124
	π-anion	Lysb55
BRD4	Van der Waals	Hısc225, Aspc317, Phec231, Argc490, Phec321, Glnc189
	π-anion	Gluc223
	π-alkyl	Leuc221, Leuc224, Proc190
	pi-pi stacked	Phec193
	pi-pi T shaped	Phec193

The objective is to determine how the ligand positions itself within the binding site of the target molecule in the most favorable conformation and to calculate the binding energy. In the molecular docking study of the ligand with BRD4 and CYP11B2, the binding energies found are -8.2 and -8.1 kcal/mol, respectively. The interactions presented in Table 4. are: Van der Waals, Hydrogen Bond, Pi-anion, Pi-cation, C–H bond Pi-Pi T-shaped, Pi-Alkyl, and Pi-Stacked.

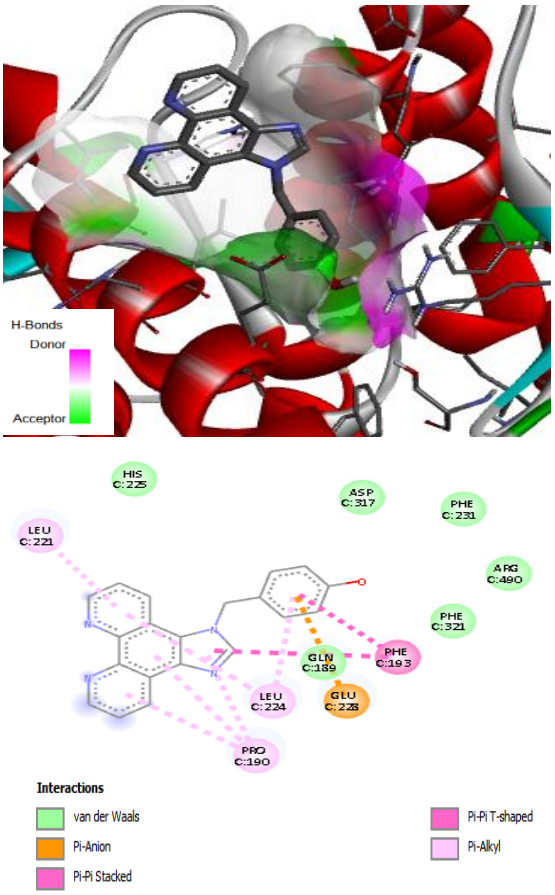


Fig. 7. *3D and 2D representation of the ligand-protein (BRD4 (*Bromodomain-Containing Protein 4*)) interaction site*

CONCLUSION

The energy of the 4-((1*H*-imidazo[4,5-*f*][1,10]phenanthrolin-1-yl)methyl)phenol ligand was minimized in the gas phase. The electronegativity, chemical potential, chemical softness, chemical hardness, and electrophilicity index of the ligand were determined using HOMO-LUMO energies. NMR and FT-IR spectra were calculated based on the optimized geometry, yielding results consistent with the relevant literature. Through molecular docking, the binding energies, interaction sites, and interaction types of the imidazophenanthroline-derivative ligand with target proteins were determined and evaluated. The information obtained here regarding the ligand will facilitate the synthesis process for the ligand, which is planned to be synthesized in the future.

REFERENCES

[1] Gök L, Turkmen H. Half-sandwich h6-areneeruthenium(II) complexes bearing 1-alkyl (benzyl)-imidazo[4,5-f][1,10]-phenanthroline (IP) derivatives: the effect of alkyl chain length of ligands to catalytic activity. Tetrahedron 2013;69:10669-10674.

[2] Gratal P, Arias-P´erez MS, Gude L. 1H-imidazo [4,5-f] [1,10] phenanthroline carbohydrate conjugates: synthesis, DNA interactions and cytotoxic activity. Bioorganic Chemistry 2022; 125:105851.

[3] Sun DD, Wang WZ, Mao JW, Mei WJ, Liu J. Imidazo[4,5-f][1,10] phenanthroline derivatives as inhibitor of c-myc gene expression in A549 cells via NF-B pathway. Bioorg Med Chem Lett 2012;22:102–105.

[4] Bergamo A, Dyson PJ, Sava G. The mechanism of tumour cell death by metal-based anticancer drugs is not only a matter of DNA interactions. Coordin Chem Rev 2018;360:17–33.

[5] Kar B, Das U, De SD, Pete S, Sharma AS, Nilmadhab R, Ashok Kumar SK, Panda D, Paira P. GSH-resistant and highly cytoselective ruthenium(ii)-p-cymene-(imidazo[4,5-f][1,10] phenanthrolin-2-yl)phenol complexes as potential anticancer agents. Dalton Trans 2021;50:10369–10373.

[6] De S, Kumar RS, Gauthaman A, Ashok Kumar SK, Paira P, Moorthy A, Banerjee S. Luminescent ruthenium(II)-para-cymene complexes of aryl substituted imidazo-1,10-phenanthroline as anticancer agents and the effect of remote substituents on cytotoxic activities. Inorgan Chim Acta 2021;515:120066.

[7] Lin J, Zhou S, Xian H, Chen W, Zhang Y, Zhang W, Guan Z, Mei W.Imidazolebased phenanthroline derivatives induce DNA damage-mediated apoptosis to suppress hepatocellular carcinoma. J Holis Integ Pharm 2022;3(2):177–189.
[8] Foresman JB, Frisch AE. Exploring chemistry with electronic structure methods (2 ed.). Wallingford, CT: Gaussian, Inc., 1996.
[9] Altürk S, Avcı D, Tamer Ö, Atalay Y.1H–pyrazole–3–carboxylic acid: Experimental and computational study. Journal of Molecular Structure 2018;1164:28-36.
[10] Manikandan M, Rajesh P, Ramasamy P. Crystal growth, structural, optical, vibrational analysis, Hirshfeld surface and quantum chemical calculations of 1 , 3, 5-triphenylbenzene single crystal. Journal of Molecular Structure 2019;1195:659-669.
[11] Singaravelan K, Chandramohan A, Madhankumar S, Enoch MV, Vinitha G. Structural characterization, computational and biological studies of a new third order NLO (1:1) organic adduct: 2-Aminopyrimidine: 3-nitrophthalic acid. Journal of Molecular Structure 2019;1194:57-65.
[12] Uluçam G, Bagcı U, Şuekinci Yılmaz A, Yentürk B. Schiff-base ligands containing phenanthroline terminals: Synthesis, characterization, biological activities and molecular docking study. Spectrochimica Acta Part A: Molecular and Biomolecular Spectroscopy 2022;279:121429.
[13] Turkyilmaz M, Uluçam G, Aktaş Ş, Okan SE. Synthesis and characterization of new N-heterocyclic carbene ligands: 1, 3-Bis (acetamide) imidazol-3-ium bromide and 3-(acetamide)-1-(3-aminopropyl)-1H-imidazol-3-ium bromide. Journal of Molecular Structure 2017;1136:263-270.
[14] Morris GM, Huey R, Lindstrom W, Sanner MF, Belew RK, Goodsell DS, Olson AJ. AutoDock4 and AutoDockTools4: Automated docking with selective receptor flexibility, J Comput Chem 2009;30:2785–2791.
[15] Salam S, Jat RK. Imidazole phenanthroline derivatives: A promising application in modern medicine. Journal of Drug Delivery and Therapeutics 2025;15(6):102-110.
[16] Andeko SB, Scott EE. Aldosterone Synthase Structure With Cushing Disease Drug LCI699 Highlights Avenues for Selective CYP11B Drug Design. Hypertension 2021;78(3):751-759.
[17] Masand VH, Rastija V. PyDescriptor: A new PyMOL plugin for calculating thousands of easily understandable molecular descriptors. Chemometrics Intelligent Laboratory Systems 2017;169:12–18.